Proceedings of the 25th International Conference on
**Port and Ocean Engineering under Arctic Conditions**
June 9-13, 2019, Delft, The Netherlands

# The strength and the physical properties of glacier-ice runways

Maren S. Kallelid[1], Torodd S. Nord[2], Sven Lidström
[1] Multiconsult AS, Tromsø, Norway
[2] Department of Civil and Environmental Engineering, Trondheim, Norway
[3]Norwegian Polar Institute, Operations and Logistics Department, Tromsø, Norway

## ABSTRACT

A field investigation program was carried out in February 2018 on the glacier-ice runway of Troll Airfield, Queen Maud Land, Antarctica. The physical properties and the strength of two types of ice were studied: glacier ice (also called blue ice) and ice used to repair melt holes (patch ice). These melt holes (cryoconites) were created by sand accumulation on the runway surface. The strength was measured using a borehole jack (BHJ). The ice temperature varied from -2°C to -15°C, with majority of the tests conducted in the colder range. The strength was measured at two depths: 10 cm and 20 cm. The cold ice was generally stronger than the warm ice, and the patch ice was in general weaker than the blue ice. The difference seemed to be related to the sun radiation and the ice temperature, and the observed failure mode shifted from ductile to brittle with decreasing ice temperature.

Ice samples were brought back to NTNU in Trondheim for further investigations of the physical properties. The density was determined through X-ray images provided by a CT scan and was found to be 845 kg $m^{-3}$ for blue ice and 898 kg $m^{-3}$ for patch ice. X-ray images of samples collected in front of the indenter revealed that air pockets in the damaged zone had been closed during indentation. Thin sections of the two ice types showed that both ice types had a granular structure, yet the blue ice had more equally sized grains of 4-5 mm whereas the grains of the patch ice ranged from 1-7 mm. Thin sections of the indented ice adjacent to the piston were investigated and compared to the failure behaviour in the loading curves from the corresponding BHJ. The data suggested that the thickness of the damaged zones was related to type of brittle failure mode.

KEY WORDS: Borehole jack; Thin sections; X-ray images; Glacier ice; Field work

## INTRODUCTION

Troll Station is a Norwegian research station located in Queen Maud Land in Antarctica, operated by the Norwegian Polar Institute (NPI). The station experienced great improvements in 2005, which included the construction of a 3 km long runway to allow for intercontinental flights with wheeled aircraft (NPI, 2007). This airstrip is quite unique in the sense of its construction material of glacier ice. In Antarctica there are currently only 11 intercontinental airfields that allows for wheeled aircraft to land. 8 of these are on ice, either glacial ice, ice shelf or sea ice.

The runway at the Troll Airfield is prone to melt holes on the surface as a result of sand accumulation from surrounding mountains (also called cryoconite holes). The dark colour of the sand particles implies that the material has a low albedo and thereby absorbs heat from the sun radiation. Melt holes can therefore be produced for temperatures below 0°C (MacDonell and Fitzsimons, 2008). The runway is frequently repaired by removing refrozen meltwater and particles in the bottom of the hole in exchange of a crushed ice-water mixture. This method is referred to as patching (NPI, 2007).

The personnel at Troll Airfield spend numerous hours during the summer season to repair the runway surface. The patching method has been successfully applied for many years, but there exist little knowledge about the strength and characteristics of the patch ice, nor the original glacier ice.

A comprehensive field investigation program was completed in February 2018, where the aim was to map the ice characteristics of the runway, and to investigate the strength properties of the ice. The results from this field work, with associated analyses, became the foundation for the master thesis of Kallelid (2018), and parts from which this paper is based upon. Measurements of air temperature, ice temperature and ice density were conducted alongside borehole jack (BHJ) indentation tests, Russian penetrometer tests, thin sections and CT-tomography scanning of collected ice cores.

In what follows, it is elaborated on the observed failure modes and recordings provided by the BHJ. Further, it is showed how the ice material adjacent to the BHJ indenter were modified.

## BOREHOLE JACK AND INDENTATION TESTS

A borehole jack (BHJ) is a mechanical device used to characterize the *in situ* strength of ice, also called the borehole ice strength. The main advantage of this test is that the tested ice is not removed from its original location, whereas the main disadvantage is the unclear stress state of the ice. Direct comparison between the strength values obtained from BHJ tests and from triaxial experiments conducted in laboratory is challenging. Sinha (2011) went as far as calling the BHJ strength an "index". Despite that the term strength obtained from BHJ experiments violates the conditions of being a material property, we use the strength term throughout the paper in order to be consistent with available BHJ literature (Sinha (2011), Timco and Weeks (2010), Johnston et al. (2003), Masterson (1996)). Also note that the term stress is herein the measured force divided by indenter area, hence in a strict sense, it is the average pressure across the indenter, but termed stress to be consistent with existing BHJ literature.

Sinha (2011) described four common stress-displacement curves, and suggested a strength definition for each. For load curves with a distinct stress peak, also called asymptotic failure, the strength value is reported as the maximum recorded stress. For curves where the stress increased continually, the reached stress value after a certain displacement should be used as the reported strength.

Johnston et al. (2003) collected data from six studies and investigated the relationship between in-situ borehole strength and the corresponding ice temperature measurements. The study combine results from second-year and multi-year ice with salinity in the range of 0 to 6.2 ‰. Despite considerable scatter in the data, they found that the ice temperature had a noticeable weakening effect on the ice strength for temperatures warmer than -5 °C.

The borehole jack may be considered as an indentation test under unknown and uncontrollable confinement. Indentation tests under controlled environment are therefore relevant for the understanding of processes ongoing adjacent to the borehole-strength indenter. Numerous examples exist of small scale indentor experiments performed on fresh water ice in cold laboratories. Some of these elaborate on the failure mode and microstructural modifications in the damaged ice adjacent to the indentor and their variation due to change in ice temperature and indentation rate.

Jordaan (2001), on the other hand, studied the compressive failure of ice through medium scale indentation tests, performed on icebergs in the field. He discovered that compressive forces were transmitted to the ice in concentrated areas called “high-pressure zones”, and that the ice material response depended on the stress distribution within the zone. The material in the central zone experienced high confinement which resulted in recrystallization, whereas the material along the edge of a pressure zone was prone to microfracturing due to lower confining pressure. Further, he emphasized that ice compressive failures consisted of cracks and spalls. He observed that ice of various sizes (up to 20 m) were ejected and broken off from the test ice specimens because of local fracture propagating from the contact zone towards the free surface. The released pieces of ice will be referred to as spalls in the following.

Barrette et al. (2002) performed small scale indentation tests in cold laboratories. They confirmed the findings related to the distribution of the microstructural modifications in the layer presented by Jordaan (2001). Furthermore, they studied how the severity of recrystallization or the microcracks in the layer were related to ice temperature. In near-melting temperatures, a majority of the damaged zone underwent a grain refinement, whereas for colder temperatures, several large zones of microfracturing where discovered in the layer.

Preceding the work of Barrette et al. (2002), Browne et al. (2013) studied the relationship between the ice failure mode and the associated load curves, and investigated how ice temperature effected the failure behaviour in the loading curves. The warm ice experiments showed ductile behaviour in which the slopes of the load curves had a smooth shape. Thin sections of the respective damaged zones revealed a heavily recrystallized area. The recorded load curves from colder ice measurements had a regular cyclic loading pattern, and the damage zone was again dominated by microfracturing. Browne et al (2013) suggested, in agreement with the data from Barrette et al. (2002), that -10 °C is the optimal temperature to obtain dynamic response in the loading curve, whereas warmer temperatures produced ductile behaviour and colder temperature produced regular cyclic loading behaviour. All tests were performed with a constant indentation rate of 4 mm $s^{-1}$.

Wells et al. (2011) suggested to divide the ice failure modes into five different behaviours: ductile behaviour, localized spall, isolated crushing events, cyclic-load crushing events and mixed mode. Note that the term localized spall herein is used to describe a sharp drop in the loading pattern, which is a result from a single flake spalling event. The severity of the failure

behaviours was ranked on a scale from 0 to 3 for each recording. All experiments were conducted at constant temperature of -10 ℃, while the indentation rate varied from 0.2 to 10 mm $s^{-1}$. The ductile failure behaviour dominated in the load curves for the slowest tests at 0.2 mm $s^{-1}$, while the brittle failure behaviours such as localized spalls, cyclic-load crushing and mixed mode appeared with increasing intensity as the indentation rate was increased. Isolated crushing events never dominated the loading curves, but appeared with highest frequency for indentation rates at 2-5 mm $s^{-1}$.

O'Rourke et al. (2016) conducted indentation tests with a compliant beam subjected to single indenters, and studied what Wells et al. (2011) referred to as brittle failure behaviours, but used terms as spalling events, sawtooth loading and lock-in conditions. They concluded that the regular sawtooth loading contributed to layer production (increasing the thickness of the damaged zone), while spalling events occurred intermittently and resulted in reduction of the contact area. The spalling event is herein both referring to removal of a relatively large piece of ice and to a sharp drop in the loading pattern. The vibrations in the lock-in failure mode corresponded to the natural frequency of the structure, and they further suggested that this failure mode contributed to vibrations within the layer rather than layer production. Hence, when the indentation rate increased, the failure mode went from sawtooth loading to a lock-in condition and the layer production was diminished.

## FIELD PROGRAM

### Borehole jack experiments

The borehole jack (BHJ) is a single-indentor system which with an 18V Makita hand drill supplies an average indentation rate of ~ 0.9 mm $s^{-1}$. Pictures of the equipment with component names are given in Fig. Figure 1. The piston diameter and the full stroke length are both 30 mm. The indentation force is provided by an 18 V Makita drill, and the movement of the piston is controlled by the forward/reverse function on the drill. A detailed description of the mechanical principles of the borehole jack is given in Kallelid (2018). A 12 mm threaded steel rod is located inside the cylinder. Upon loading, a triangular steel bracket attached to the end of the steel rod is dragged upwards inside the cylinder. This movement pushes the indenter into the ice as the piston slides along the angled side of the triangle. Two load cells are located in between the handle and the top plate, and the vertical force needed to pull the triangular bracket upwards are registered as compressive forces in the cylinder by the load cells. The indentation force can be calculated based on the steel bracket geometry and assumed friction coefficients. However, a calibration tool has been developed to determine the exact relationship between the measured force and the actual indentation force.

The BHJ experiments were carried out along the runway and at the airport apron of Troll Airfield. In total 65 BHJ experiments were conducted in the period of 9.-23. February, 2018. The experiments were organized in smaller areas spread along the airstrip and at the apron. 3 to 8 experiments were conducted within each testing area with an internal spacing of approximately 2 meters. The experiments were conducted in both blue ice and patch ice. The blue ice measurements were performed at depth 10 cm and 20 cm, while the patch ice measurements were all conducted at 10 cm (limited by the depth of the patches). Hence, the experiments are divided into three groups: $patch_{10}$, $blue_{10}$, and $blue_{20}$ with 11, 45 and 9 recordings in each group, respectively.

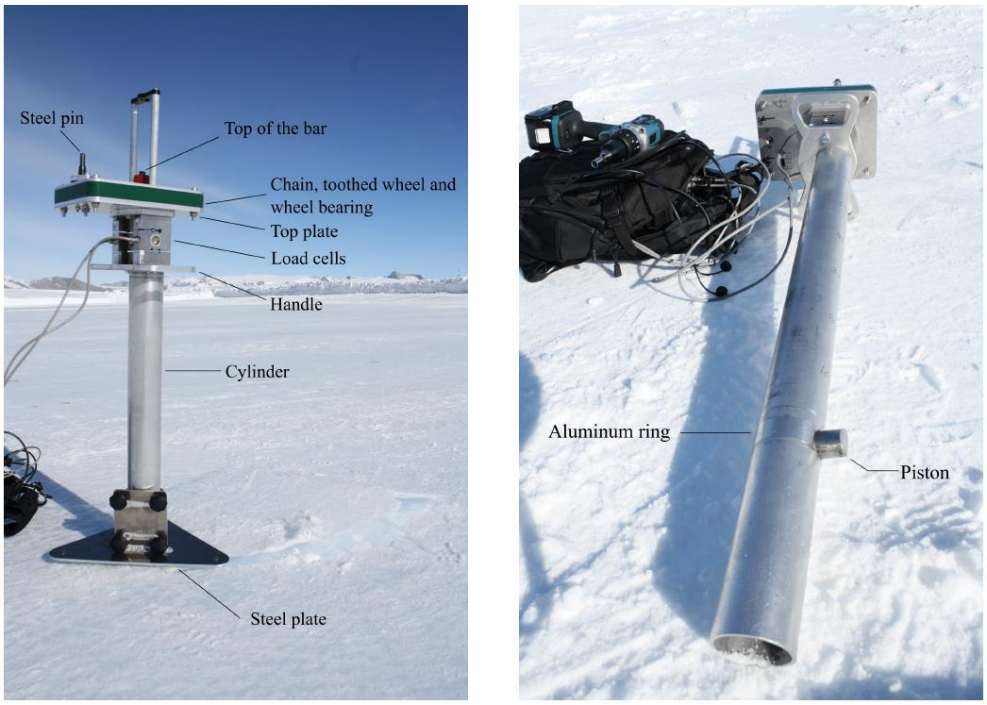


*Figure 1: Photographs of the borehole jack. The most important components of the equipment are pointed out. A Makita drill is used to spin the steel pin.*

After each recording, the ice temperature and the size of the spall (if any) was measured and sounds from the ice during the indentation was noted. Additionally, the weather conditions and air temperature were reported on a daily basis.

**Thin sections and CT scan**

Ice samples were collected at Troll Airfield and transported to NTNU (Trondheim, Norway) for further investigations. The ice was sampled using a Kovacs drill with 75 mm diameter and an electric bolt threading machine. Blue ice was collected at both ends and the middle of the runway, from depth ~ 5-25 cm. One patch ice sample was collected at the airport apron from depth ~5-10 cm. In addition, three ice cores of indented ice adjacent to the piston were collected. It was only possible to sample indented ice from $blue_{20}$ recordings because these tests were the only ones were spalling did not occur and the ice was relative intact. A Cool-Ice freezing box with several cooling elements was used to transport the ice cores from Troll to NTNU.

At NTNU, the ice core samples were investigated, first through CT scanning and afterwards through thin sectioning. The CT scan performed at NTNU is an X-ray computed microtomography scan which provides cross-sectional pictures of the whole ice core.

After the CT scan was completed, the ice cores were cut in slabs for thin section preparations. Both vertical and horizontal thin sections were made when the size of the ice core allowed it. Regarding the indented ice samples, the cuts were made so as to intersect the centre of the indentation zone. The thin sections were produced by a method where both sides of the sections were polished. Photographs were taken of the sections when located in between cross-polarized filters with background light. For a more detailed description of the CT scan and the thin sectioning method, see Kallelid (2018).

## RESULTS AND DISCUSSION

A summary of the results from the Troll field work program is presented in this section. See Kallelid (2018) for a comprehensive and more detailed presentation of all the collected results. Note that a calibration tool for the borehole jack has been developed after the test campaign. Calibration at temperatures ranging from 0 °C to -20 °C showed that the ratio between vertical force measured by the load cells and the horizontal force from the piston ranged from 1.8 to 2.3. In this paper, a constant value of 1.99 is used, which was based upon hand calculations and assumed friction coefficients.

### Borehole jack

Examples of typical stress-time curves recordings from depth 10 cm and 20 cm are given in Fig. 2a) and 2b), respectively. In this paper, the strength of the ice is defined as the maximum recorded stress, according to the definition used for premature failure presented by Sinha (2011). For simplicity, this definition is used for all the recordings, despite that the stress in several of the *blue*$_{20}$ recordings tends to increase continually or level off, and a "yield strength" would be more appropriate. The difference in terminal stress behaviour is reflected in the failure mode observations in the field. For most of the tests performed at depth 20 cm, no spalls nor cracks were visible at the surface, and the stress levelled off as illustrated in Fig. 2b). For the shallower tests at depth 10 cm, a spall was consequently produced, and a distinct stress peak as the one in Fig. 2a) could be seen in the stress curves. The diameter of these spalls ranged from 15 cm to 85 cm. It was observed that tests performed in warm ice (temperatures warmer than -5 °C) produced relatively small spalls. For tests performed in colder ice, the spall size appeared to be more random. In addition, the ice adjacent to the piston mark was visually inspected in the field. A powder-like material was observed in the piston-ice intersection.

The ice strength for all recordings are plotted against the ice temperature in Fig. 3a). The results suggest that increasing temperatures weakened the ice strength. This tendency is particular evident for the measurements conducted at 20 cm depth (marked by squares in Fig 3a), which

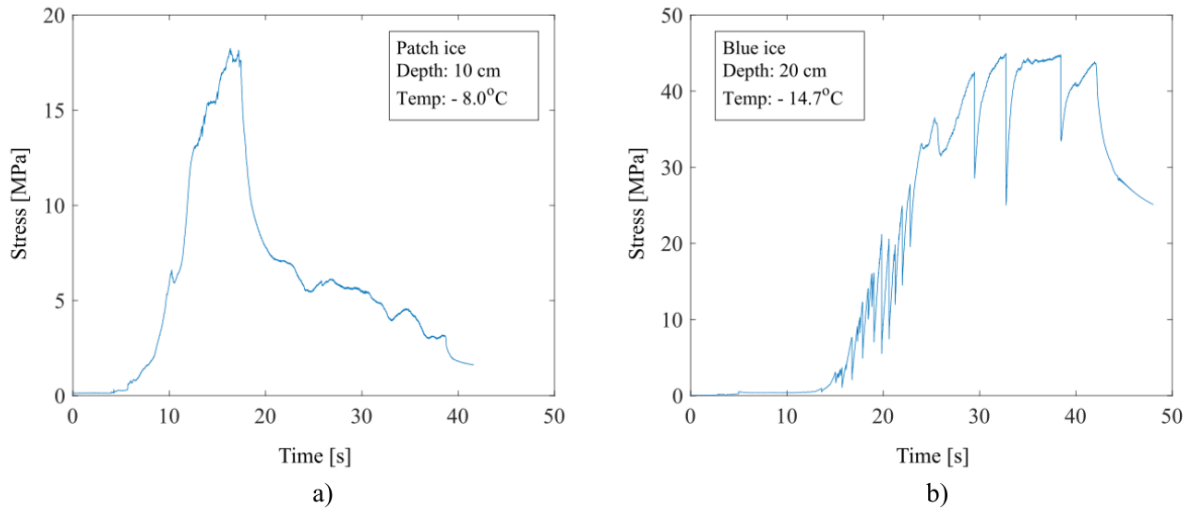


*Figure 2: Typical stress-time curves from BHJ recordings. a)* Patch$_{10}$ *recording. Premature failure with ductile failure behaviour in the stress curve. One isolated crushing event can be observed at approximately 10 sec. b)* Blue$_{20}$ *recording. "Yield strength"-example where the stress levels off at a plateau. Initially the failure behaviour is mixed mode (or sawtooth loading). Three localized spalling events can be observed at the plateau.*

was conducted in a temperature range of -9 to - 5°C. For multi-year ice, Johnston et al. (2003) suggested that the ice temperature had the most significant strength effect when the ice temperature approached near-melting temperatures. Too few measurements were conducted in tempered ice during our field work to draw conclusions about weakening effects of the glacier ice strength at near-melting temperatures.

The maximum recorded stress in measurements conducted at 20 cm depth were in general higher than the shallower measurements. The resistance at depth 20 cm is higher due to higher confinement and longer distance towards the free surface than at depth 10 cm. The higher degree of confinement at 20 cm depth also made this ice less sensitive towards natural, localized flaws in the ice, thereby causing less scatter in strength values.

Attempts to find spatial variability of the strength along the runway length were also conducted, yet no systematic variability was found.

Regarding the engineering challenges at the runway concerning melt ponds and patches, a comparison of the recordings from the blue ice and the patch ice is highly relevant. When investigating the strength and temperature data, it is discovered that the patch ice is in general warmer than the blue ice, and that the measured strength values of the patch ice is lower than the blue ice strength values. On the first testing day, one could feel the sun heating, and on this particular day, the patch ice temperature was considerably higher than the blue ice temperature. A report of the daily, average blue ice, patch ice and air temperature is given in Kallelid (2018). Further, the recorded patch ice strength values from the first day was considerable lower than the blue ice strength measurements from the same day. It seems that sun radiation heats the patch ice and thereby reduces the ice strength. This phenomena might be explained by dark particles in the patch ice, left in the bottom of the cryoconite during the reparation process. The patch ice was often visually darker than the blue ice, and after conduction of a BHJ experiment, one could often observe small amounts of sand particles underneath the spall. The low albedo of these dark particles leads to heat absorption from the sun and increases the patch ice temperature (MacDonell and Fitzsimons, 2008).

The influence of temperature onto the failure behaviour is herein studied by means of the classification as suggested by Wells et al. (2011). This classification divides the failure behaviours into five categories by means of time histories of the load; ductile behaviour, localized spall, isolated crushing events, cyclic-load crushing events and mixed mode. Fig. 2a)

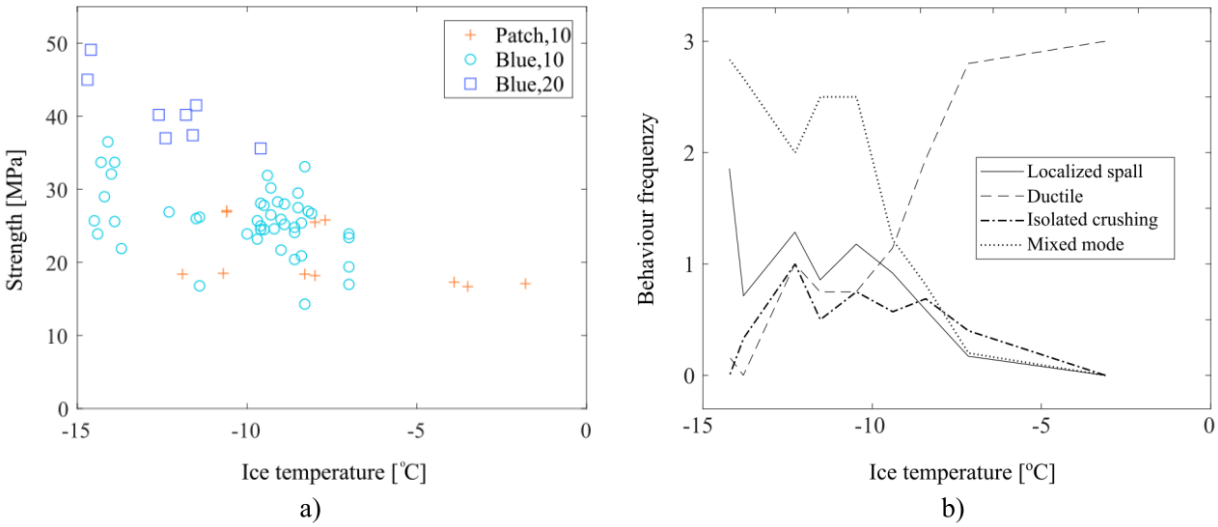


*Figure 3: a) Ice strength vs. ice temperature. b) Failure behaviour evolution for decreasing temperatures.*

shows an example of ductile behaviour with one isolated crushing event, and Fig. 2b) illustrates mixed mode in the first part of the curve and localized spalls in the later part. Cyclic loading events as described by Wells et al. (2011) are not observed in any of the BHJ curves. The severity of each failure behaviour in the stress curves are ranked from 0 to 3 for all the $blue_{10}$ and $patch_{10}$ recordings. Note that this analysis is only based on a visual inspection of the stress-time histories, as inspection of the actual indentation zone for all tests was considered too time consuming. The $blue_{20}$ recordings are excluded in this comparison due to the higher degree of confinement. The plot in Fig. 3b) shows how the severity index evolves with decreasing ice temperature. The evolution proves to follow the same pattern as observed by Wells et al. (2011) when constant ice temperature and increasing indentation rate was applied. The ductile failure behaviour dominates in the higher temperature range, with decreasing intensity as the temperature gets colder. The brittle failure behaviours, as localized spalls and mixed modes are almost non-existing in the higher temperature range, whereas the severity increases at the temperature gets colder. Isolated crushing events never dominates, yet the frequency is highest in the medium temperature range.

Sawtooth loading, as described by O'Rourke et al. (2016), is observed sporadic in the stress curves for recordings conducted in cold temperatures. However, the difference between mixed mode, sawtooth loading and cyclic loading events is unclear, and whether the oscillations in the slopes are regular enough to be described as sawtooth loading is up for discussion. The sawtooth loading may also be triggered by the flexibility of the BHJ.

It must be noted that even though most of the experiments were conducted with optimal cyclic loading ice temperatures at approximately -10°C (Browne et al, 2013), the BHJ indentation rate of ~ 0.9 mm $s^{-1}$ is considerably lower than the indentation rates used in the comparison experiments. Hence, the results presented in this paper are in general of a less brittle manner than results presented in other papers.

During the BHJ indentation tests, different sounds could be heard, varying from long-lasting squeeze-sounds to periodic crushing-sounds. Often loud, distinct crack sounds was heard. Whenever these crack sounds were counted, the number of load drops in the stress curves (localized spalls) matched the counted crack sounds.

**Thin sections and CT-scan**

The thin sections of the blue ice show that the glacier ice has a granular structure with grain size mainly in the range of 4-5 mm. Two examples of blue ice horizontal and vertical cut thin sections are displayed in Fig. 4a) and 4b), respectively. Some of the vertical sections show a tendency of a vertical grain elongation, as exemplified by Fig. 4b). It is not observed any structural variation in the sections with depth, nor any spatial variation along the runway length.

Fig. 4c) shows a picture of a horizontal cut thin section of patch ice. This thin section also indicates a granular, isotropic structure, yet the grain sizes vary over a larger range from 1-7 mm.

The three samples of the ice adjacent to the indenter were examined through both thin sections and a CT scan. Fig. 5 shows photographs of the thin sections with cross polarized light (left), X-ray pictures from the CT scan (middle) and the stress-time curve from the corresponding

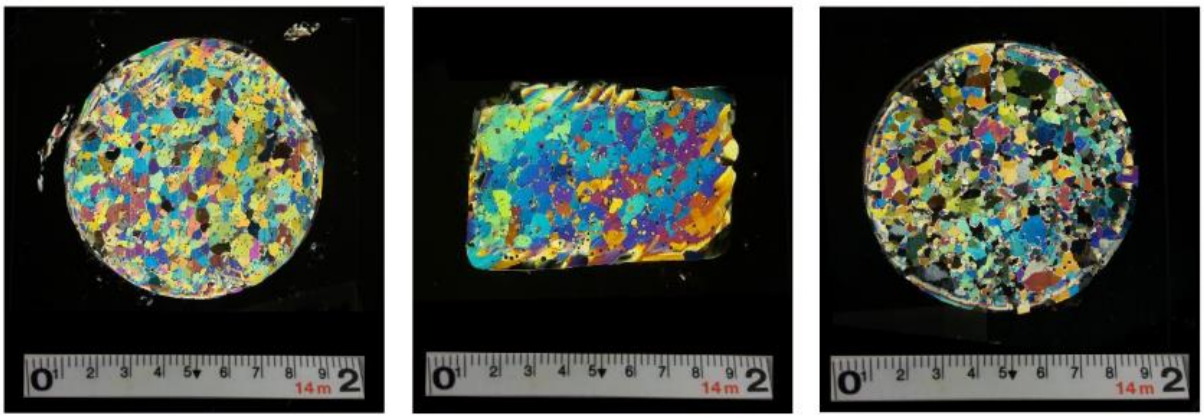


*Figure 4: Thin sections of blue ice and patch ice photographed when located in between cross-polarized filters with back lightning. a) Blue ice, depth 10 cm, horizontal cut. b) Blue ice, depth 20 cm, vertical cut. c) Patch ice, depth 5 cm, horizontal cut*

BHJ recording (right). Thin sections in (a) and (c) are vertical cuts and (b) is a horizontal cut. All the X-ray pictures represent horizontal cross sections, and the red dashed lines in a) and c) indicate the locations of the vertical thin sections.

The blue lines in the thin section photographs mark the contact area between the indenter and the ice, and since the sections are not cut from the middle of the indented mark, the blue lines are not the fully length of the 30 mm piston diameter. The red lines indicate the transition between the damaged layer and the intact blue ice and was used to measure the layer thickness. The layer thickness was estimated: a) 2 cm, b) 0.4 cm and c) 1.5 cm, with some inherent uncertainties caused by inaccuracy of the sample cut procedure. The appraisal of the damaged zone is simply based on a visual inspection. The distribution of recrystallization and microcracks in the layer were not studied in this project.

O'Rourke et al. (2016) suggested that sawtooth loading contributes to layer production and spalling reduces the contact area. The results presented in Fig. 5 support this statement: The stress-time curve with the greatest severity of sawtooth loading (a) is the recording that produced the largest damaged zone, and the curve in (b) is dominated by localized spalls, and the corresponding damaged zone is the thinnest. However, due to the uncertainties in the layer thickness measurements as explained above, these results are only indicative and need further investigation.

The X-ray pictures in the middle column of Fig. 5 enable a study of the air bubble distribution in the indented ice. The grey colour represents ice material, and the black dots represent air. It appears from the pictures that the air content is considerable lower in the areas corresponding to the damaged zones found in the thin sections. The air bubbles have in all likelihood been closed during the indentation, an observation which to the author's knowledge has not been reported elsewhere. This adds to the already well known ice layer responses to the microstructural modifications already described in literature. The closing air bubbles adjacent to the indenter would imply that the density of the material changes during interaction, and how this may change for 1) different types of ice (i.e. sea ice), and 2) during a cycle of ice-induced vibrations is still unknown. A few, narrow stripes of air are partly visible in the damaged layers, plausible from air bubbles that have only been partly closed. The stripes within the same area are directed parallel to each other and might imply the direction of the local compressive forces.

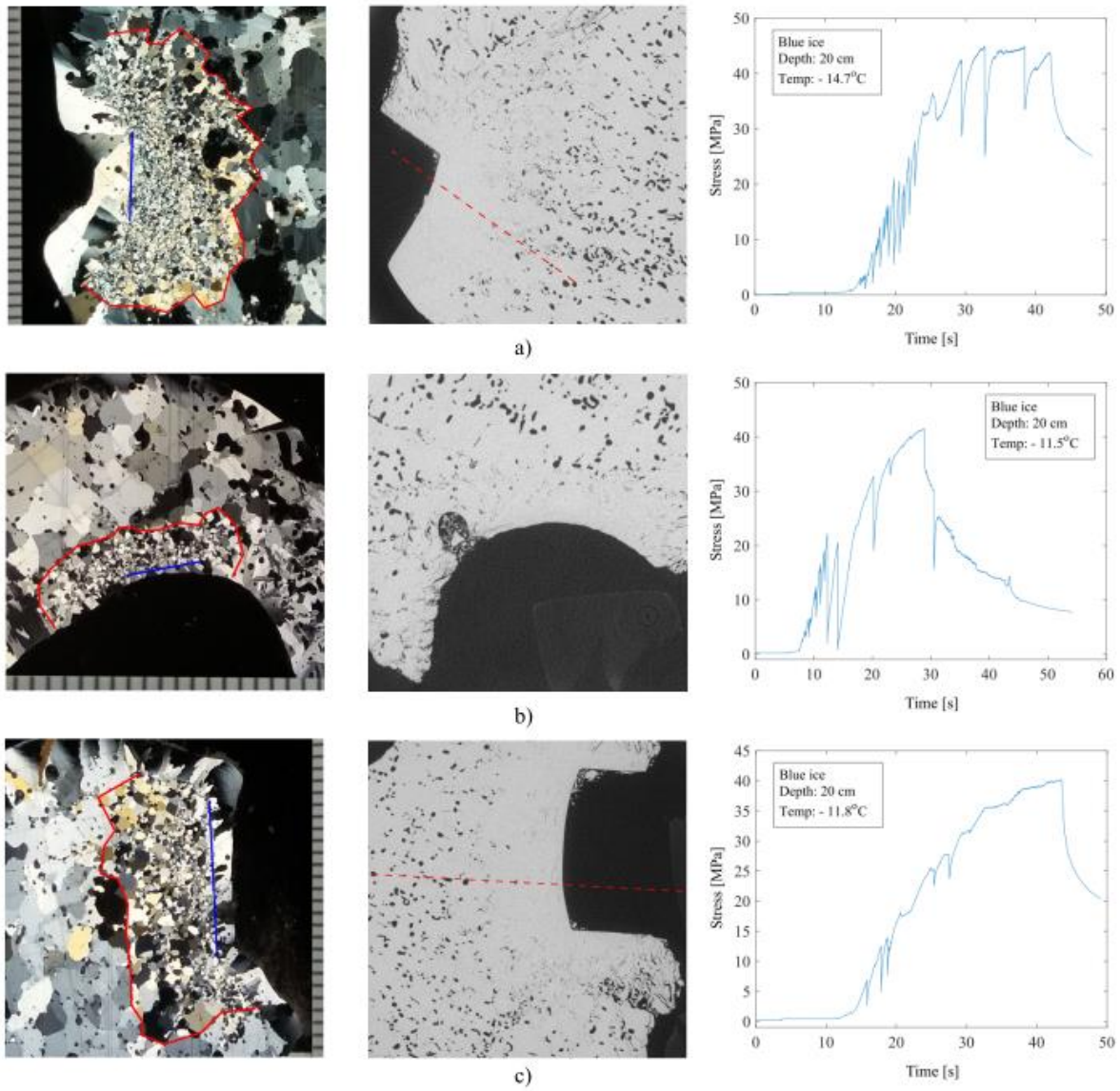


*Figure 5: Comparison of thin section photographs of indented ice (left), CT scan pictures (middle) and stress-time curve (right). a), b) and c) represents thee different* $blue_{20}$ *recordings. The thin section pictures from a) and c) are vertical cuts, while b) is a horizontal cut. The red line marks the transition from the damage zone and the intact blue ice, and the blue line indicates the piston mark. All CT scan pictures are horizontal, and the red dashed line indicates the location of the vertical thin section cut. The spacing of the ruler in the thin section pictures is 2 mm.*

## Density

The density was measured in field using the mass/volume method. However, the results from this method showed a considerable scatter in density values and will therefore not be further utilized.

The density is also calculated based on the solid volume fraction, found by computer analysis of the X-ray pictures provided by the CT scan. The blue ice density is found to be 845 kg $m^{-3}$ and the patch ice density is found to be 898 kg $m^{-3}$.

## CONCLUSIONS

The field work at Troll Airfield was conducted to investigate the blue ice and patch ice properties of the ice pavement at the runway. A summary of the obtained characteristics for the two ice types is given in Tab. 1.

Table 1. Characterization of the blue ice and the patch ice

| Characteristics | Blue ice | Patch ice |
|---|---|---|
| Density | 845 kg $m^{-3}$ | 898 kg $m^{-3}$ |
| Structure | Granular | Granular |
| Grain size | 4-5 mm | 1-7 mm |
| Grain elongation | Moderate vertical elongation | None |

Based on the analysis of the BHJ experiments, the thin sections and the CT scan, the following conclusions can be drawn:

- The results from the strength measurements indicate that heat has a weakening effect on the ice, as the recorded strength in tempered ice was in general lower than cold ice measurements.
- The patch ice temperature was often higher than the blue ice temperature and the warmer ice was weaker than the cold ice. The temperature difference seemed to increase whenever there was a noticeable heat from the sun. The reason for this variation in temperature is plausible dark particles left in the patches, which absorb heat from sun radiation and increases the patch ice temperature.
- The evolution of the failure behaviour in the stress curves follow the same pattern for reduced ice temperatures as Wells et al. (2011) found for increasing indentation rates.
- X-ray pictures from CT scanning indicate that the air bubbles in the damaged zone have been closed during the indentation.

## ACKNOWLEDGEMENTS

This project was supported by Norwegian Polar Institute Operations and Logistics Department. The authors wishes to thank the staff at Troll Station and Troll Airfield for their support and hard work.

## REFERANCES

Barrette, P., Pond, J., Jordaan, I., 2002. Ice damage and layer formation in small-scale indentation experiments. In: Ice in the Environment: *Proceedings of the 16th IAHR International Symposium on Ice, Dunedin, New Zealand, Dec. 2–6, 2002. Vol. 3*, pp.246–253.

Browne, T., Taylor, R., Jordaan, I., Gürtner, A., 2013. Small-scale ice indentation tests with variable structural compliance. *Cold Regions Science and Technology*, 88, pp.2–9.

Johnston, M., Timco, G. W., & Frederking, R., 2003. In situ borehole strength measurements on multi-year sea ice. In: *The Thirteenth International Offshore and Polar Engineering Conference.* International Society of Offshore and Polar Engineers.

Jordaan, I. J., 2001. Mechanics of ice–structure interaction. *Engineering Fracture Mechanics*, 68 (17-18), 1923–1960.

Kallelid, M. S., 2018. *A study of the strength and physical properties of glacier ice.* MSc. Trondheim: Norwegian University of Science and Technology.

MacDonell, S., Fitzsimons, S., 2008. The formation and hydrological significance of cryoconite holes. *Progress in Physical Geography,* 32 (6), pp.595–610.

Masterson, D. M., 1996. Interpretation of in situ borehole ice strength measurement tests. *Canadian Journal of Civil Engineering*, 23.1, pp.165-179.

O'Rourke, B. J., Jordaan, I. J., Taylor, R. S., Gürtner, A., 2016. Experimental investigation of oscillation of loads in ice high-pressure zones, part 1: Single indentor system. *Cold Regions Science and Technology,* 124, pp.25–39.

Sinha, N. K., 2011. Borehole indentor-a tool for assessing in-situ bulk ice strength and micromechanics. *Cold Regions Science and Technology*, 69 (1), pp.21–38.

Norwegian Polar Institute (NPI), 2007. *Technical Report on Troll Airfield, Dronning Maud Land, Antarctica*, Tromsø: NPI

Timco, G., Weeks, W., 2010. A review of the engineering properties of sea ice. *Cold regions science and technology*, 60 (2), pp.107–129.

Wells, J., Jordaan, I., Derradji-Aouat, A., Taylor, R., 2011. Small-scale laboratory experiments on the indentation failure of polycrystalline ice in compression: Main results and pressure distribution. *Cold Regions Science and Technology,* 65 (3), pp.314 – 325.